Simulation-Based Design Optimization by Sequential Multi-criterion Adaptive Sampling and Dynamic Radial Basis Functions

Matteo Diez, Silvia Volpi, Andrea Serani, Frederick Stern and Emilio F. Campana

Abstract The paper presents a global method for simulation-based design optimization (SBDO) which combines a dynamic radial basis function (DRBF) surrogate model with a sequential multi-criterion adaptive sampling (MCAS) technique. Starting from an initial training set, groups of new samples are sequentially selected aiming at both the improvement of the surrogate model global accuracy and the reduction of the objective function. The objective prediction and the associated uncertainty provided by the DRBF model are used by a multi-objective particle swarm optimization algorithm to identify Pareto-optimal solutions. These are used by the MCAS technique, which selects new samples by down-sampling the Pareto front, allowing for a parallel infill of an arbitrary number of points at each iteration. The method is applied to a set of 28 unconstrained global optimization test problems and a six-variable SBDO of the DTMB 5415 hull-form in calm water, based on potential flow simulations. Results show the effectiveness of the method in reducing the computational cost of the SBDO, providing the background for further developments and application to more complex ship hydrodynamic problems.

1 Introduction

Simulation-based design optimization (SBDO) techniques have developed in the last decades in response to the high cost of the build-and-test design paradigm, relying on the increasing accuracy of the simulation tools and availability of computational resources. SBDO requires the automated integration of design modification tools, accurate computer simulations, and optimization algorithms. SBDO typically

M. Diez (✉) · A. Serani · E. F. Campana
CNR-INSEAN, National Research Council-Marine Technology Research Institute,
Via di Vallerano 139, 00128 Rome, Italy
e-mail: matteo.diez@cnr.it

S. Volpi · F. Stern
IIHR–Hydroscience and Engineering, The University of Iowa 100 C. Maxwell
Stanley Hydraulics Laboratory, Iowa City 52242-1585, USA

requires a large number of computer simulations to identify the global optimal solution to the design problem. The high-fidelity, complexity, and computational expense of the simulation tools is approaching resource saturation, requiring therefore cost-reducing solutions.

The application of surrogate models alleviate the computational cost of SBDO. When performing surrogate-based SBDO, a sampling of the design space by design of experiment (DoE) techniques is used to train a surrogate model of the desired objective function, which is used by the optimization algorithm. Surrogates have been widely used in performing SBDO, including optimization of stochastic black-box functions [14], optimization under uncertainty [15], sampling-based reliability-based design optimization [31], deterministic [5] and stochastic [10] hydrodynamic optimization.

The sampling of the design space needs to be efficient an effective, possibly achieving two competitive goals: an adequate global accuracy of the surrogate model (especially when a global optimum is sought), and a fine investigation of promising design regions [2]. DoEs defined on the basis of a priori methods can hardly achieve these goals. For this reason, *adaptive* sampling techniques have been developed which exploit information that becomes available during the optimization process. The literature proposes a large variety of adaptive sampling criteria. Some examples include: the Kushner's criterion [19], which maximizes the probability of improving the objective; the expected improvement criterion, used in the efficient global optimization (EGO) algorithm [16]; the lower confidence bounding function [7], which minimizes the linear combination of surrogate model prediction and surrogate model uncertainty; locating the threshold-bounded extreme, locating the regional extreme, and minimizing surprises [30].

The objective of the current research is the extension of a dynamic radial basis function (DRBF) surrogate model [29], used in earlier work for uncertainty quantification of ship hydrodynamic problems, to global, derivative free, deterministic design optimization.

The current method implements a sequential *multi-criterion adaptive sampling* (MCAS) technique based on DRBF-predicted objective and associated uncertainty. Starting from an initial training set, groups of new samples are selected from the Pareto front of non-dominated solutions obtained by a multi-objective extension of the deterministic particle swarm optimization (MODPSO) algorithm [4, 18, 22]. An additional single-objective DPSO [26] is performed over the DRBF model to improve the selection of the global minimizer. The procedure is iterated until convergence.

The method is applied to 28 unconstrained global optimization test problems, as well as to the hull-form optimization in calm water and fixed speed of the DTMB 5415, an early concept of the USS Arleigh Burke-class destroyer DDG-51 used as a benchmark for experimental [20, 27] and numerical optimization [12, 13, 25] studies. A potential flow code [1] is used for the simulations. The performance of the DRBF method is assessed by comparison with a direct application of DPSO.

2 Optimization Problem Formulation

Given a design variable vector $\mathbf{x}$ of dimension N and a design objective

$$f(\mathbf{x}) \ : \ \mathbb{R}^N \to \mathbb{R} \tag{1}$$

the optimization problem is formulated as

$$\min_{\mathbf{x} \in \Omega} f(\mathbf{x}) \tag{2}$$

where

$$\Omega = \left\{ \mathbf{x} \in D \subset \mathbb{R}^N \mid c_i(\mathbf{x}) \le 0, \ \ i = 1, \dots, N_c \right\} \tag{3}$$

is the feasible set, D is the design space defined by box constraints, and $c_i(\mathbf{x})$ are inequality constraints. Herein, these are handled by a linearly penalized objective function

$$f_p(\mathbf{x}) = f(\mathbf{x}) + \gamma \sum_{i=1}^{N_c} \max \left[c_i(\mathbf{x}), 0 \right] \tag{4}$$

3 Dynamic Radial Basis Function Method for Optimization

3.1 Surrogate Model

Given a set of M training points $\{\mathbf{z}_i\}_{i=1}^M$ with associated function evaluations $y_i = g(\mathbf{z}_i)$, a power law RBF provides predictions as

$$h(\mathbf{x}, \varepsilon_j) = \sum_{i=1}^M w_i \varphi \left(||\mathbf{x} - \mathbf{z}_i|| \right) \quad \text{with} \quad \varphi = ||\mathbf{x} - \mathbf{z}_i||^{\varepsilon_j} \tag{5}$$

where the exponent $\varepsilon_j \in \mathbb{R}$ is a tuning parameter; $\mathbf{w} = \{w_i\}_{i=1}^M$ is the solution of the linear system that provides exact prediction at $\mathbf{x} = \mathbf{z}_i$

$$\mathbf{A}\mathbf{w} = \mathbf{y} \quad \text{with} \quad a_{ij} = \varphi \left(||\mathbf{z}_i - \mathbf{z}_j|| \right) \quad \text{and} \quad \mathbf{y} = \{y_i\} \tag{6}$$

The DRBF model [29] provides the expected value of a sample of RBF predictions over a stochastic distribution of ε_j. Herein, ε_j is assumed uniformly distributed between $\varepsilon_{\min}$ and $\varepsilon_{\max}$:

$$\hat{g}(\mathbf{x}) = \text{EV}[h(\mathbf{x}, \varepsilon_j)] \quad \text{with} \quad \{\varepsilon_j\}_{j=1}^{N_\varepsilon} \sim \text{unif}[\varepsilon_{\min}, \varepsilon_{\max}] \tag{7}$$

The uncertainty $\hat{U}_g(\mathbf{x})$ associated to the prediction at $\mathbf{x}$ is quantified by the 95%-confidence band of $h(\mathbf{x}, \varepsilon_j)$.

If multiple functions $(g_k, k = 1, \ldots, N_g)$ are assessed, multiple surrogate models need to be computed. If these are based on the same training points $\{\mathbf{z}_i\}_{i=1}^M$, with corresponding function evaluations $\mathbf{y}_k = \{g_k(\mathbf{z}_i)\}_{k=1}^{N_g}$, a single factorization of the matrix $\mathbf{A}$ may be used. In fact, the system

$$\mathbf{AW} = \mathbf{Y} \tag{8}$$

may be solved at once. In this case, $\mathbf{W} = \begin{bmatrix} \mathbf{w}_1 | \ldots | \mathbf{w}_{N_g} \end{bmatrix}$ and $\mathbf{Y} = \begin{bmatrix} \mathbf{y}_1 | \ldots | \mathbf{y}_{N_g} \end{bmatrix}$.

When the surrogate model is used for unconstrained optimization, $N_g = 1$, $g(\mathbf{x}) = f(\mathbf{x})$, and the model output is the couple $\{\hat{f}, \hat{U}_f\}$. When the surrogate model is used for constrained optimization, $N_g = N_c + 1$, $g_1(\mathbf{x}) = f(\mathbf{x})$, $g_2(\mathbf{x}) = c_1(\mathbf{x})$, ..., $g_{N_c+1}(\mathbf{x}) = c_{N_c}(\mathbf{x})$, and the output is the $N_c + 1$ couples $\{\hat{f}, \hat{U}_f\}$, $\{\hat{c}_1, \hat{U}_{c_1}\}$, ..., $\{\hat{c}_{N_c}, \hat{U}_{c_{N_c}}\}$. The penalized objective function $\hat{f}_p(\mathbf{x})$ is computed using the predictions $\hat{f}, \hat{c}_1, \ldots, \hat{c}_{N_c}$, as per Eq. 4.

3.2 Multi-criterion Adaptive Sampling

Starting from an initial training set, the MCAS identifies groups of new samples balancing the surrogate model accuracy and the search for the global minimizer. This is pursued by solving the multi-objective optimization problem

$$\min_{\mathbf{x} \in D} \hat{f}_p(\mathbf{x}) \quad \text{and} \quad \max_{\mathbf{x} \in D} \hat{U}_f(\mathbf{x}) \tag{9}$$

Note that for unconstrained problems $\hat{f}_p(\mathbf{x})$ corresponds to $\hat{f}(\mathbf{x})$, while $\hat{U}_f(\mathbf{x})$ is always the uncertainty of the (non-penalized) objective.

The Pareto front obtained is down-sampled in order to identify m equally spaced points along a curvilinear coordinate ξ (Fig. 1). In view of the fact that: (a) sampling too close to available training points does not add useful information to the analysis, (b) as the distance between training points decreases, the matrix A in Eq. 6 may result ill-conditioned, and (c) the uncertainty at the training points is zero, i.e.

$$\lim_{||\mathbf{x}-\mathbf{z}_i|| \to 0} \hat{U}_f(\mathbf{x}) = 0, \tag{10}$$

a constraint is defined such that $\hat{U}_f(\mathbf{x}) \geq u_{\min}$, where $u_{\min} = \beta \hat{U}_{range}$ with $\hat{U}_{range} = \{\max[\hat{U}_f(\mathbf{x})] - \min[\hat{U}_f(\mathbf{x})]\}$.

Fig. 1 Pareto solutions of
the multi-objective problem
with samples
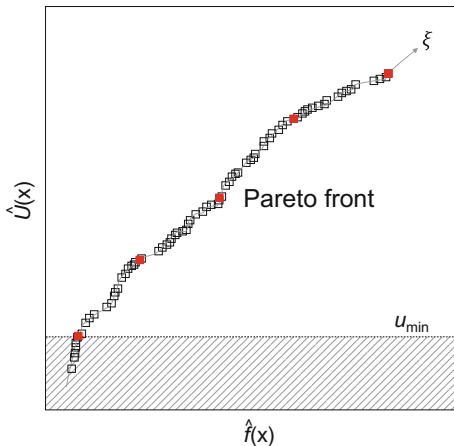
3.3 Optimization Procedure

The optimization procedure using DRBF and MCAS is performed as per the following algorithm.

Algorithm DRBF with MCAS

Step 1. Define an initial DoE $\{\mathbf{z}_i\}_{i=1}^M$ and evaluate objective function and constraints $\mathbf{Y} = [\mathbf{y}_1 | \ldots | \mathbf{y}_{N_c+1}]$.

Step 2. Initialize the current optimum: $y_{\text{opt}} = \min(\mathbf{y}_1)$ and $\mathbf{x}_{\text{opt}} = \text{argmin}(\mathbf{y}_1)$.

Step 3. Build the DRBF model for objective and constraints $\{\hat{f}, \hat{U}_f\}, \ldots, \{\hat{c}_{N_c}, \hat{U}_{c_{N_c}}\}$ using the training set $T \equiv \{\mathbf{z}_i, \mathbf{Y}_{ik}\}$.

Step 4. Find the minimizer $\mathbf{x}^*$ of $\hat{f}_p(\mathbf{x})$ by DPSO and compute the true objective function $y^* = f(\mathbf{x}^*)$.

Step 5. If $y^* < y_{\text{opt}}$ then
　　　update the current optimum $\mathbf{x}_{\text{opt}} = \mathbf{x}^*$.

Step 6. If $\hat{U}_f(\mathbf{x}^*) \geq u_{\min}$ then
　　　add $\tilde{\mathbf{z}}_1 = \mathbf{x}^*$ to the new DoE;
　　　define a new DoE $\{\tilde{\mathbf{z}}_i\}_{i=2}^m$ by MCAS;
　　　evaluate objective and constraints at $\{\tilde{\mathbf{z}}_i\}_{i=2}^m$.
　　Else
　　　define a new DoE $\{\tilde{\mathbf{z}}_i\}_{i=1}^m$ by MCAS;
　　　evaluate objective and constraints at $\{\tilde{\mathbf{z}}_i\}_{i=1}^m$.

Step 7. Add the new m samples to T.

Step 8. Iterate step 3 to 7 until convergence.

---

4 Deterministic Particle Swarm Optimization

Particle Swarm Optimization (PSO) belongs to the class of heuristic algorithms for single-objective evolutionary derivative-free global optimization and was originally introduced by Kennedy and Eberhart [18]. In order to make PSO more efficient for its use within SBDO, a deterministic version of the algorithm (DPSO) was formulated by Campana et al. [4] as follows

$$\begin{cases} \mathbf{v}_i^{k+1} = \chi \left[\mathbf{v}_i^k + c_1(\mathbf{x}_{i,pb} - \mathbf{x}_i^k) + c_2(\mathbf{x}_{gb} - \mathbf{x}_i^k) \right] \\ \mathbf{x}_i^{k+1} = \mathbf{x}_i^k + \mathbf{v}_i^{k+1} \end{cases} \tag{11}$$

Equation 11 represents velocity and position, respectively, of the ith particle at the kth iteration. Particles are attracted by the personal best position $\mathbf{x}_{i,pb}$ ever found by the ith particle and by the global best position $\mathbf{x}_{gb}$ ever found by all particles. The effectiveness of DPSO depends on the constriction factor χ, the cognitive and social learning rate c_1 and c_2, along with the number of individuals N_p and their initial distribution and velocity. Serani et al. [26] investigate the effect of such parameters and propose guidelines for an efficient use of the algorithm in the context of ship hydrodynamic optimization [24].

The extension of DPSO to multi-objective problems can be found, for instance, in Pellegrini et al. [22]. This is based on extending the definition of the personal and global best in the Pareto-optimality sense. Specifically, the personal attractor $\mathbf{x}_{i,pb}$ is the closest point to $\mathbf{x}_i$ of the pesonal Pareto front. The global attractor $\mathbf{x}_{i,gb}$ is different for each particle and defined as the closest point to $\mathbf{x}_i$ of the global Pareto front.

5 Optimization Problems

The DRBF model with the MCAS method is applied to unconstrained global optimization test problems and to the hull-form optimization of the DTMB 5415. The formulation of the problems is presented in the following.

### 5.1 Unconstrained Global Optimization Test Problems

The study includes the minimization of 28 unconstrained global optimization test problems [3, 29] with a number of independent variables ranging from two to 12. These include multimodal, highly nonlinear, and transcendental functions. Table 1 provides details of the problems, such as their dimension and search domain.

Table 1 Unconstrained global optimization test problems

Function	No. variables	ID	Bounds
Alpine	2, 3, 4, 6, 12	A2, A3, A4, A6, A12	$-10 \leq x_i \leq 5$
Exponential	2, 3, 4, 6, 12	E2, E3, E4, E6, E12	$-10 \leq x_i \leq 5$
Griewank	2, 3, 4, 6, 12	G2, G3, G4, G6, G12	$-5 \leq x_i \leq 5$
Hartmann	3, 6	H3, H6	$0 \leq x_i \leq 1$
Levy	2, 3, 4, 6, 12	L2, L3, L4, L6, L12	$-10 \leq x_i \leq 10$
McCormick	2	M2	$-1.5 \leq x_1 \leq 4,$ $-3 \leq x_2 \leq 4$
Styblinski-Tang	2, 3, 4, 6, 12	S2, S3, S4, S6, S12	$-5 \leq x_i \leq 5$

5.2 Hull-Form Optimization of the DTMB 5415

The SBDO example is the hull-form optimization of the DTMB 5415 model (Fig. 2). This has been widely investigated by towing tank experiments [20, 27] and SBDO studies [12, 17, 25, 28]. In the present work, a single-objective SBDO is shown, aiming at the reduction of the total resistance R_T in calm water at 18 kn, corresponding to a Froude number (Fr) equal to 0.25. Main particulars and design conditions are summarized in Table 2.
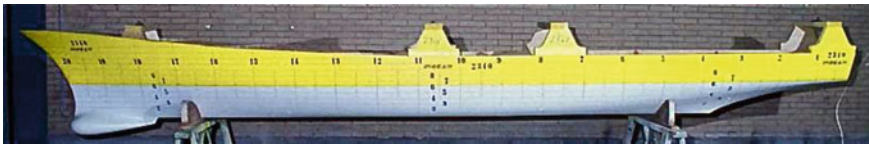
Fig. 2 A 5.720 m length model of the DTMB 5415 (CNR-INSEAN model 2340)

Table 2 DTMB 5415 model main particulars and test conditions (full scale)

Description	Symbol	Unit	Value
Displacement	∇	Tonnes	8,636
Length between perpendiculars	LBP	m	142
Beam	B	m	18.9
Draft	T	m	6.16
Longitudinal center of gravity	LCG	m	71.6
Vertical center of gravity	VCG	m	1.39
Speed	V	kn	18
Water density	ρ	kg/m^3	998.5
Kinematic viscosity	ν	m^2/s	1.09×10^{-6}
Gravity acceleration	g	m/s^2	9.803

An orthogonal representation of the shape modification is used, since more efficient in the context of shape design optimization [3, 9]. Specifically, six orthogonal functions $\Psi_{1,\dots,6}$ are applied for the modification of the hull shape, controlled by six design variables $\alpha_{1,\dots,6}$:

$$
\begin{cases}
\Psi_j(u, v) := \alpha_j \sin\left(\dfrac{p_j \pi u}{A_j} + \phi_j\right) \sin\left(\dfrac{q_j \pi v}{B_j} + \chi_j\right) \mathbf{e}_{k(j)} \\
(u, v) \in [0; A_j] \times [0; B_j]
\end{cases}
\tag{12}
$$

where u and v are curvilinear coordinates; p_j and q_j define the order of the function in u and v direction, respectively; ϕ_j and χ_j are the corresponding spatial phases; A_j and B_j define the modification domain size; $\mathbf{e}_{k(j)}$ is a unit vector. Table 3 summarizes the parameters used here, including upper and lower bounds of α_j. The results will be presented in terms of non-dimensional design variables $x_j \in [-1, 1]$ given by $x_j = 2(\alpha_j - \alpha_{j,min})/(\alpha_{j,max} - \alpha_{j,min}) - 1$. Geometrical constraints include fixed displacement and length between perpendiculars (automatically satisfied by the geometry modification tool), and $\pm 5\%$ maximum variation of beam and draft.

The solver used is the potential flow code WARP [1] based on the double model linearization [8]. The wave resistance is estimated by integrating the pressure over the hull, whereas the friction resistance is estimated by a local approximation based on flat-plate theory [23]. Simulations are performed for the right demi-hull taking advantage of the symmetry about the xz plane. The computational domain for the free surface is defined within 1 LBP upstream, 3 LBP downstream and 1.5 LBP sideways. The associated panel grid used can be found in Serani et al. [25]. The validation of the computations for the original hull is shown in Fig. 3 versus experimental data collected at CNR-INSEAN [21] showing a reasonable agreement especially for low speeds. $C_T = R_T/0.5\rho V^2 S_{w,\text{stat}}$, δ, and τ are shown, where R_T is the total resistance, $S_{w,\text{stat}}$ is the static wetted surface area, δ is the sinkage (positive if the center of gravity sinks), and τ is the trim (positive if the bow sinks).

Table 3 Orthogonal function parameters for shape modification

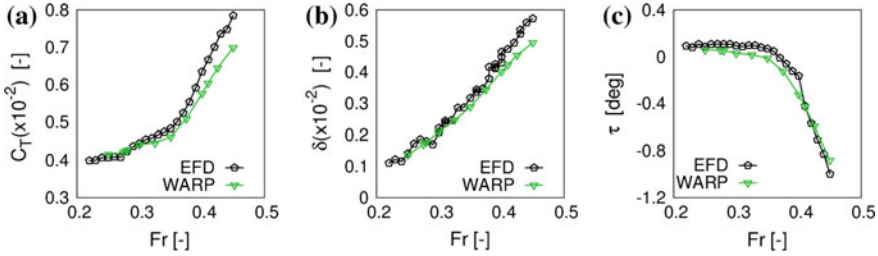| Description	j	p_j	ϕ_j	q_j	χ_j	$k(j)$	$\alpha_{j,min}$ (m)	$\alpha_{j,max}$ (m)
Hull modification	1	2.0	0	1.0	0	2	−1.0	1.0
	2	3.0	0	1.0	0	2	−1.0	1.0
	3	1.0	0	2.0	0	2	−0.5	0.5
	4	1.0	0	3.0	0	2	−0.5	0.5
Sonar dome modification	5	1.0	0	1.0	0	2	−0.3	0.3
	6	0.5	$\pi/2$	0.5	0	3	−0.5	0.5

Fig. 3 Total resistance coefficient (**a**), non-dimensional sinkage (**b**), and trim (**c**) in calm water versus Fr, for the model scale DTMB 5415 (*LBP* = 5.72 m)

6 Numerical Results

The test problems are solved using the following setup. The initial DoE is a Hammersley sequence sampling (HSS), $N_\varepsilon = 513$, $\varepsilon \in [0.75, 2.5]$, $m = 5$, $\beta = 0.01$, and the maximum number of function evaluations N_{eval} is 1000. The hull-form optimization is solved using the following setup. The initial DoE is a HSS, $N_\varepsilon = 200$, $\varepsilon \in [0.75, 2.5]$, $m = 8$, $\beta = 0.01$, and $N_{eval} = 1000$. DPSO parameters are given in Table 4.

6.1 Unconstrained Global Optimization Test Problems

For the assessment of the test problems, the normalized difference between the current optimum and the true minimum Δ_f is used as a metric [3]. DRBF and DPSO are iterated until $\Delta_f \leq 0.1\%$ or until the number of function evaluations reaches N_{eval}.

Figure 4 shows the convergence of DRBF and DPSO algorithms for the test problems E2, H6, and G12 as an example. The figure displays the value of the metric versus the number of functions evaluations M. DRBF is found significantly more effective than DPSO for E2 and G12, and slightly more efficient for H6. The average performance of DRBF and DPSO is summarized in Fig. 5, taking into account all the test problems. The average number of function evaluations needed to achieve $\Delta_f \leq 0.1\%$ is shown versus the number of design variables N. On average, DRBF

Table 4 DPSO parameters

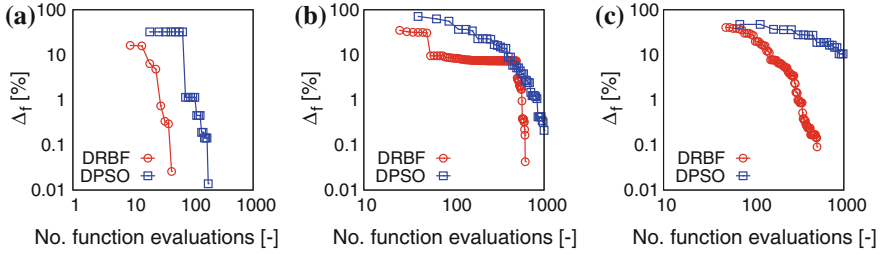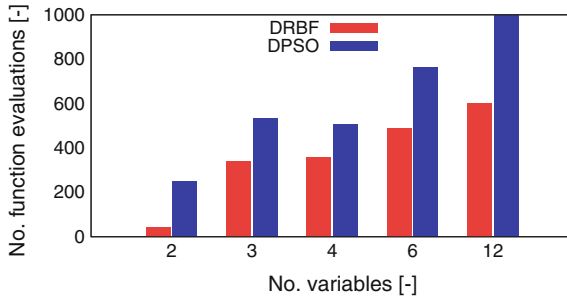| Objective function	N_p	N_{eval}	Initialization	$[\chi \quad c_1 \quad c_2]$
f_p (no surrogate)	$4N$	1000	HSS $\mathbf{v} \neq 0$ [5]	[0.721 1.655 1.655] [6]
$\hat{f}_p$ (surrogate, single-objective)	$4N$	$256N$	HSS $\mathbf{v} \neq 0$ [5]	[0.721 1.655 1.655] [6]
$\hat{f}_p, \hat{U}_f$ (MCAS, multi-objective)	$32N$	$1024N$	HSS $\mathbf{v} = 0$	[0.9801 0.3333 0.6767] [11]

Fig. 4 Convergence of DRBF and DPSO for test problems E2 (**a**), H6 (**b**), G12 (**c**)

Fig. 5 Average number of function evaluations needed to achieve $\Delta_f \leq 0.1\%$
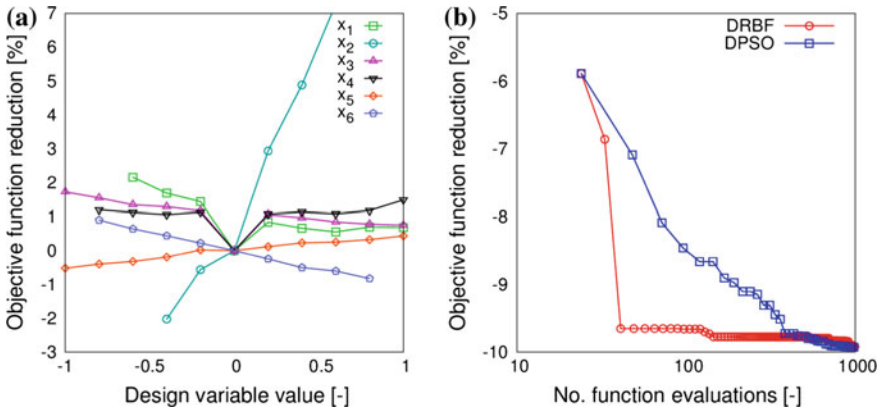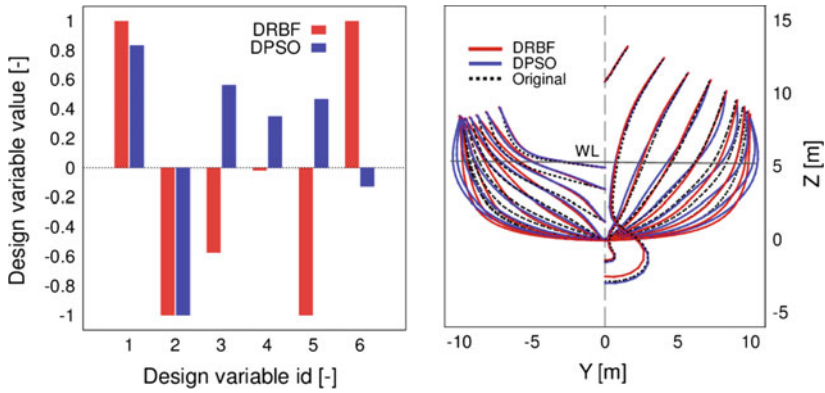

Fig. 6 Sensitivity analysis of the design variables (**a**), and convergence of DRBF and DPSO for the hull-form optimization of the DTMB 5415 (**b**)
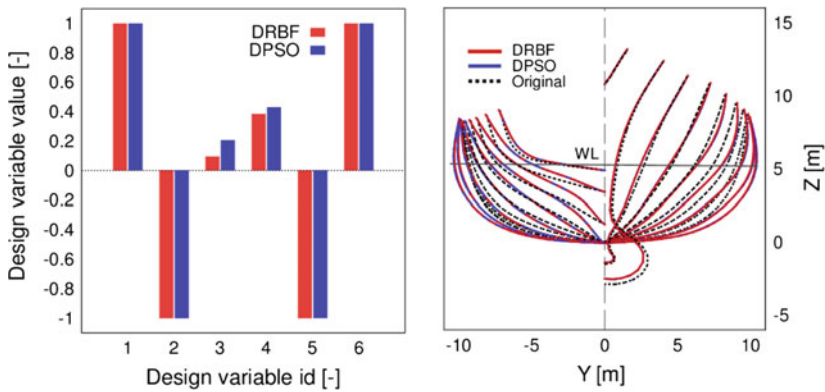
requires fewer function evaluations to achieve the optimal solution. Moreover, DRBF outperforms DPSO for $N = 12$ since the latter does not achieve $\Delta_f \leq 0.1\%$ for any of the problems within the prescribed budget N_{eval}.

(a) 50 function evaluations
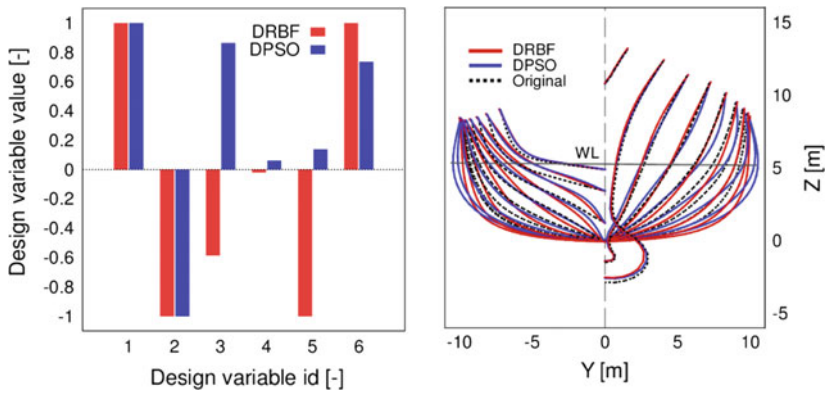
(b) 100 function evaluations

(c) 1000 function evaluations

Fig. 7 Optimal design variables (left), and sections of the DTMB 5415 original and optimized hulls, comparing DRBF and DPSO solutions (right)

Table 5 Design variables and objective function values for the DTMB 5415 hull-form

No. function evaluations		Design variables [–]						$R_T \times 10^5$ [N]	
		x_1	x_2	x_3	x_4	x_5	x_6	Value	$\Delta\%$
50	DRBF	1.00	−1.00	−0.57	−0.02	−1.00	1.00	3.07	−9.65
	DPSO	0.83	−1.00	0.56	0.35	0.47	−0.13	3.16	−7.09
100	DRBF	1.00	−1.00	−0.59	−0.02	−1.00	1.00	3.07	−9.66
	DPSO	1.00	−1.00	0.86	0.06	0.14	0.74	3.11	−8.46
1000	DRBF	1.00	−1.00	0.10	0.38	−1.00	1.00	3.06	−9.92
	DPSO	1.00	−1.00	0.21	0.43	−1.00	1.00	3.06	−9.93

6.2 Hull-Form Optimization of the DTMB 5415

The penalized objective of Eq. 4 is computed using a penalty coefficient $\gamma = 100$.

A preliminary sensitivity analysis for each design variable is presented in Fig. 6a. Unfeasible designs are not reported. Changes in f reveal a potential reduction of the total resistance (at Fr = 0.25) close to 2%.

The optimization process by DRBF is shown in Fig. 6b, including the comparison with DPSO. The figure displays the convergence of f versus M. Note that all the solutions correspond to feasible designs. Both methods reach a total resistance reduction
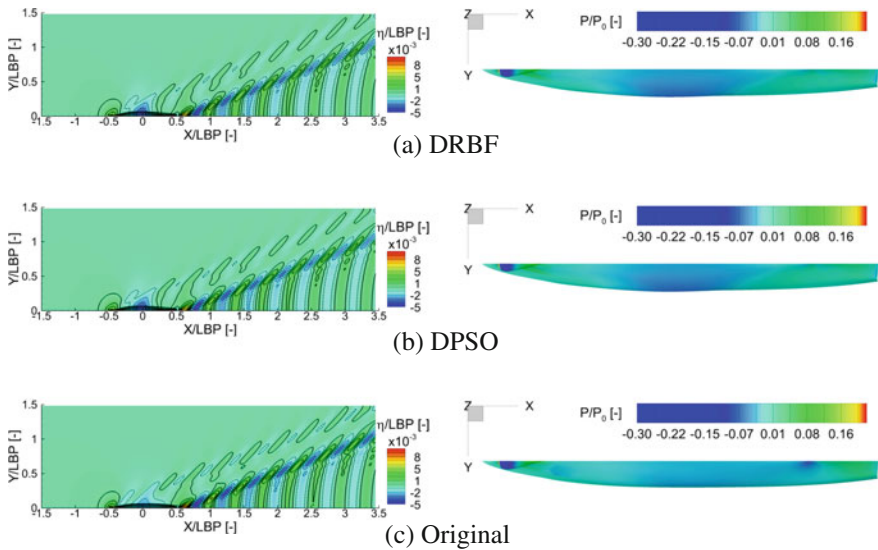

Fig. 8 Wave elevation pattern (left) and pressure field distribution (right) at Fr = 0.25 of the optimized DRBF (**a**) and DPSO (**b**) hulls compared to the original (**c**), with 1000 function evaluations

Table 6 Summary of optimization results for DTMB 5415 hull-form

Parameter	Unit	Original	Optimized $\Delta\%_{\text{orig}}$	
			DRBF	DPSO
C_w	–	1.00E−03	−26.36	−26.77
C_f	–	1.61E−03	−0.04	−0.05
C_T	–	2.62E−03	−10.15	−10.30
δ/LBP	–	1.37E−03	5.45	5.27
τ	rad	9.90E−04	91.54	89.99
$S_{w,\text{stat}}/LBP^2$	–	1.48E−01	0.25	0.42
$S_{w,\text{dyn}}/LBP^2$	–	1.51E−01	0.36	0.52

close to 10%. DRBF provides a quite sudden convergence achieving 9.6% reduction with 41 function evaluations, whereas DPSO requires nearly 400 evaluations to reach the same improvement.

Figure 7a, b, and c show the solutions for 50, 100, and 1000 function evaluations, respectively, in terms of variable values and hull sections of the corresponding designs. Table 5 gives the design variables and the associated objective function values. The solutions provided by DRBF and DPSO differ in the objective reduction by 2.66%, 1.20%, and 0.01%, for 50, 100, and 1000 evaluations, respectively.

Figure 8 shows the non-dimensional wave elevation pattern and the associated non-dimensional pressure distributions on the hull comparing DRBF and DPSO final designs to the original hull. The transverse wave is reduced and the pressure shows a better recovery towards the stern.

Finally, Table 6 summarizes the main parameters associated with the optimal DRBF and DPSO designs. The resistance coefficients are defined as $C_x = R_x/0.5 \rho V^2 S_{w,\text{stat}}$, with R_w, R_f, R_T being wave, frictional, and total resistance, respectively; $S_{w,\text{stat}}$ and $S_{w,\text{dyn}}$ are static and dynamic wetted surface areas.

7 Conclusions and Future Work

The current study investigates the performance of a novel method for simulation-based design optimization (SBDO), which combines a dynamic radial basis function (DRBF) surrogate model with a sequential multi-criterion adaptive sampling (MCAS) technique. The MCAS selects groups of new samples sequentially, starting from an initial deterministic DoE and using the function prediction and its associated uncertainty as provided by the surrogate model. Function value and uncertainty of the surrogate are the two objectives of a multi-objective deterministic particle swarm optimization (MODPSO) algorithm, which is used to obtain Pareto-optimal solutions. The MCAS performs the parallel infill of an arbitrary number of new training points by down-sampling of the Pareto front. Therefore, this sampling method

pursues simultaneously the global accuracy of the surrogate and the refinement of optimal regions, also exploiting the availability of parallel computing architectures.

Numerical results for a set of 28 unconstrained global optimization test problems show that DRBF outperforms a direct application of DPSO, requiring on average approximately 80% fewer function evaluations for two-dimensional problems and 35% for higher dimensions.

The application of DRBF to the six-variable hull-form optimization of the DTMB 5415 shows the potential of the method in performing constrained SBDO problems. The hull is optimized using a potential flow solver and the total resistance is reduced by nearly 10%. For a large number of simulations, DRBF and DPSO converge approximately to the same solution. DRBF is found more efficient than the direct application of DPSO, showing a quite sudden convergence. Specifically, 9% resistance reduction is achieved by DRBF requiring nearly ten times fewer simulations than DPSO.

Future developments include the assessment of optimal initial DoEs, in terms of number of samples and distribution, along with the optimal number of samples selected by the MCAS technique at each iteration. The promising result of DRBF lays the groundwork for further investigations, including SBDO with larger design spaces and the use of high-fidelity CFD methods, such as RANS solvers.

References

1. Bassanini, P., Bulgarelli, U., Campana, E., Lalli, F.: The wave resistance problem in a boundary integral formulation. Surv. Math. Ind. **4**, 151–194 (1994)
2. Booker, A.J., Dennis Jr., J., Frank, P.D., Serafini, D.B., Torczon, V., Trosset, M.W.: A rigorous framework for optimization of expensive functions by surrogates. Struct. Optim. **17**(1), 1–13 (1999). https://doi.org/10.1007/BF01197708
3. Campana, E.F., Diez, M., Iemma, U., Liuzzi, G., Lucidi, S., Rinaldi, F., Serani, A.: Derivative-free global ship design optimization using global/local hybridization of the DIRECT algorithm. Optim. Eng. **17**(1), 127–156 (2015)
4. Campana, E.F., Liuzzi, G., Lucidi, S., Peri, D., Piccialli, A., Pinto, A.: New global optimization methods for ship design problems. Optim. Eng. **10**(4), 533–555 (2009). https://doi.org/10.1007/s11081-009-9085-3
5. Chen, X., Diez, M., Kandasamy, M., Zhang, Z., Campana, E.F., Stern, F.: High-fidelity global optimization of shape design by dimensionality reduction, metamodels and deterministic particle swarm. Eng. Optim. **47**(8), 473–494 (2015)
6. Clerc, M.: Stagnation analysis in particle swarm optimization or what happens when nothing happens (2006). http://clerc.maurice.free.fr/pso
7. Cox, D.D., John, S.: SDO: a statistical method for global optimization. In: Multidisciplinary Design Optimization: State of the Art, pp. 315–329 (1997)

8. Dawson, C.W.: A practical computer method for solving ship-wave problems. In: Proceedings of the 2nd International Conference on Numerical Ship Hydrodynamics, pp. 30–38. Berkeley (1977)
9. Diez, M., Campana, E.F., Stern, F.: Design-space dimensionality reduction in shape optimization by Karhunen-Loève expansion. Comput. Methods Appl. Mech. Eng. **283**, 1525–1544 (2015)
10. Diez, M., Chen, X., Campana, E.F., Stern, F.: Reliability-based robust design optimization for ships in real ocean environment. In: Proceedings of 12th International Conference on Fast Sea Transportation, FAST2013, Amsterdam, The Netherlands (2013)
11. Diez, M., Peri, D.: Robust optimization for ship conceptual design. Ocean Eng. **37**(11), 966–977 (2010)
12. Diez, M., Serani, A., Campana, E.F., Goren, O., Sarioz, K., Danisman, D.B., Grigoropoulos, G., Aloniati, E., Visonneau, M., Queutey, P., Stern, F.: Multi-objective hydrodynamic optimization of the DTMB 5415 for resistance and seakeeping. In: Proceedings of the 13th International Conference on Fast Sea Transportation, FAST 2015. Washington, D.C., USA (2015)
13. Grigoropoulos, G., Campana, E., Diez, M., Serani, A., Goren, O., Sarioz, K., Danisman, D., Visonneau, M., Queutey, P., Abdel-Maksoud, M., et al.: Mission-based hull form and propeller optimization of a transom stern destroyer for best performance in the sea environment. In: Michel Visonneau, P.Q., Touzé, D.L. (eds.) VII International Conference on Computer Methods in Marine Engineering, pp. 83–94 (2017)
14. Huang, D., Allen, T., Notz, W., Zeng, N.: Global optimization of stochastic black-box systems via sequential Kriging meta-models. J. Global Optim. **34**(3), 441–466. https://doi.org/10.1007/s10898-005-2454-3, http://dx.doi.org/10.1007/s10898-005-2454-3
15. Jin, R., Du, X., Chen, W.: The use of metamodeling techniques for optimization under uncertainty. Struct. Multidiscip. Optim. **25**(2), 99–116 (2003)
16. Jones, D.R., Schonlau, M., Welch, W.J.: Efficient global optimization of expensive black-box functions. J. Global Optim. **13**(4), 455–492 (1998)
17. Kandasamy, M., Wu, P.C., Zalek, S., Karr, D., Bartlett, S., Nguyen, L., Stern, F.: CFD based hydrodynamic optimization and structural analysis of the hybrid ship hull. SNAME (2014)
18. Kennedy, J., Eberhart, R.: Particle swarm optimization. In: Proceedings of IEEE Conference on Neural Networks, IV, Piscataway, NJ, pp. 1942–1948 (1995)
19. Kushner, H.J.: A new method of locating the maximum point of an arbitrary multipeak curve in the presence of noise. J. Fluids Eng. **86**(1), 97–106 (1964)
20. Longo, J., Stern, F.: Uncertainty assessment for towing tank tests with example for surface combatant DTMB model 5415. J. Ship Res. **49**(1), 55–68 (2005)
21. Olivieri, A., Pistani, F., Avanzini, A., Stern, F., Penna, R.: Towing tank experiments of resistance, sinkage and trim, boundary layer, wake, and free surface flow around a naval combatant INSEAN 2340 model. Technical report, DTIC Document (2001)
22. Pellegrini, R., Serani, A., Leotardi, C., Iemma, U., Campana, E.F., Diez, M.: Formulation and parameter selection of multi-objective deterministic particle swarm for simulation-based optimization. Appl. Soft Comput. **58**, 714–731 (2017)
23. Schlichting, H., Gersten, K.: Boundary-Layer Theory. Springer, Berlin (2000)
24. Serani, A., Diez, M.: Are random coefficients needed in particle swarm optimization for simulation-based ship design? In: Proceedings of the 7th International Conference on Computational Methods in Marine Engineering (MARINE 2017), pp. 48–59. Nantes, France (2017)
25. Serani, A., Fasano, G., Liuzzi, G., Lucidi, S., Iemma, U., Campana, E.F., Stern, F., Diez, M.: Ship hydrodynamic optimization by local hybridization of deterministic derivative-free global algorithms. Appl. Ocean Res. **59**, 115–128 (2016)
26. Serani, A., Leotardi, C., Iemma, U., Campana, E.F., Fasano, G., Diez, M.: Parameter selection in synchronous and asynchronous deterministic particle swarm optimization for ship hydrodynamics problems. Appl. Soft Comput. **49**, 313–334 (2016)
27. Stern, F., Longo, J., Penna, R., Olivieri, A., Ratcliffe, T., Coleman, H.: International collaboration on benchmark CFD validation data for surface combatant DTMB model 5415. In: Proceedings of Twenty-Third Symposium on Naval Hydrodynamics (2001)

28. Tahara, Y., Peri, D., Campana, E.F., Stern, F.: Computational fluid dynamics-based multiobjective optimization of a surface combatant using a global optimization method. J. Mar. Sci. Technol. **13**(2), 95–116 (2008)
29. Volpi, S., Diez, M., Gaul, N.J., Song, H., Iemma, U., Choi, K.K., Campana, E.F., Stern, F.: Development and validation of a dynamic metamodel based on stochastic radial basis functions and uncertainty quantification. Struct. Multidiscip. Optim. **51**(2), 347–368 (2015). https://doi.org/10.1007/s00158-014-1128-5
30. Watson, A.G., Barnes, R.J.: Infill sampling criteria to locate extremes. Math. Geol. **27**(5), 589–608 (1995)
31. Zhao, L., Choi, K.K., Lee, I., Gorsich, D.: Conservative surrogate model using weighted Kriging variance for sampling-based RBDO. J. Mech. Des. **135**(9), 091,003 (2013)